Gutenberg-Richter's law in sliding friction of gels

Tetsuo Yamaguchi[1], Masatoshi Morishita[1], Masao Doi[1], Takane Hori[2], Hide Sakaguchi[2], and Jean-Paul Ampuero[3]

Abstract. We report on experimental studies of spatio-temporally heterogeneous stick-slip motions in the sliding friction between a hard polymethyl methacrylate (PMMA, plexiglass) block and a soft poly-dimethyl siloxane (PDMS, silicone) gel plate. We perform experiments on two PDMS gels with different viscoelastic properties. For the less viscous gel, large and rapid events are preceded by an alternation of active and less active periods. For the more viscous gel, successive slow slip events take place continuously. The probability distributions of the force drop, a quantity analogous to seismic moment, obey a power law similar to Gutenberg-Richter's empirical law for the frequency-size statistics of earthquakes, and the exponents of the power law vary with the plate velocity and the viscosity of the gel. We propose a simple model to explain the dependence of the power law exponent on the plate velocity, which agrees with experimental results.

1. Introduction

Describing the spatio-temporal complexity of earthquakes is known as one of the most challenging problems to study with physics-based models due to their strong non-linearity and large number of degrees of freedom [*Strogatz*, 1994]. However, earthquake catalogs usually show a simple power-law relationship between the magnitude and the number of earthquakes, which is known as "Gutenberg-Richter's law" (GR law) [*Gutenberg and Richter*, 1965]. Numerous attempts have been made to understand the physical origins of the complexity of earthquakes and the simple scaling of the GR law [*Scholz*, 2002]. *Burridge and Knopoff* [1967] introduced a basic model (BK model) to mimic complex sequences of earthquakes that consisted of a chain of blocks elastically coupled together and to a loading plate, and subject to velocity-dependent frictional contact with a fixed plate. At that time, the number of blocks considered in the model was quite moderate due to the limited computational resources available. Therefore, spatio-temporal complexity with a broad range of scales could not be realized. Nonetheless, owing to the velocity-dependent friction, the BK model produced highly complex stick-slip motions even with only a few blocks. As a result, further efforts were focused on developing velocity-dependent frictional constitutive relationships rather than on explaining the GR law.

With the advent of the concept of self-organized criticality (SOC) [*Bak et al.*, 1987], the GR law was highlighted as a typical topic of SOC study. With the help of computer power, *Carlson and Langer* [1989] extended the BK model simulations to a larger number of blocks. They found out power-law statistics of slip events without requiring any spatial heterogeneity in their model parameters. Following their work, Olami et al. introduced a non-conservative cellular automaton model (OFC model) [*Olami et al.*, 1992; *Christensen and Olami*, 1992] that reproduced the GR law. Moreover, its exponent (called b value in seismology) was reported to vary with the amount of energy dissipation during the rupture events. In actual earthquake catalogs, the b value is significantly variable (e.g. [*Mogi*, 1967; *Utsu*, 1974; *Scholz*, 2002; *Mori and Abercrombie*, 1997; *Schorlemmer et al.*, 2005]), but the systematics and origins of such variability have not yet been elucidated.

On the other hand, attempts to understand earthquake physics through experimental approaches have been conducted for decades. Like in the BK model during its early development stage, most of the laboratory experimental studies were aimed at establishing frictional constitutive relationships for natural faults from frictional experiments on rock or gouge samples [*Dieterich*, 1978; *Dieterich*, 1979; *Ruina*, 1983; *Marone*, 1998; *Scholz*, 1998]. However, a rock specimen for frictional tests is intrinsically not suitable to mimic the rupture process with spatio-temporal complexities to investigate the physical meaning of the GR law in earthquakes, because each rupture is too large compared to the specimen size due to the stiffness of the rock. These limitations are analogous to those of a BK model with few degrees of freedom.

Unlike hard materials, soft elastic materials like rubbers or gels can produce slip events of various sizes. *Vallette and Gollub* [1993] studied the sliding friction of a thin latex membrane in contact with a translating glass rod, which is equivalent to the 1D version of the BK model. *Ciliberto and Laroche* [1994] performed friction experiments between two elastic rough surfaces. They found a power-law behavior in the statistics of slip events. Recently, the authors observed the spatio-temporal stick-slip behavior along a 2D planar interface made of an adhesive gel-sheet sliding on a glass plate [*Yamaguchi et al.*, 2009; *Morishita et al.*, 2010]. These findings suggest that soft materials such as rubbers or gels are relevant analogue materials to study spatio-temporal complexity in earthquakes.

In this paper, we report on the spatio-temporally heterogeneous stick-slip motions in the sliding friction between a hard PMMA block and a soft PDMS gel plate. In order to investigate the relationship between energy dissipation and sliding behavior or slip statistics, we performed experiments using two PDMS gels having different viscoelastic properties. The details of the experimental materials and method are described in section 2. As shown in section 3, sliding behavior is quite heterogeneous in spite of no specific quenched disorder in these systems. Significant effects

[1]Department of Applied Physics, The University of Tokyo, Tokyo, Japan.(yamaguchi@rheo.t.u-tokyo.ac.jp)
[2]IFREE, JAMSTEC, Yokohama, Kanagawa, Japan.
[3]Seismological laboratory, California Institute of Technology, Pasadena, California, USA.

0148-0227/11/$9.00

of viscous dissipations on the spatio-temporal frictional behavior are observed: the slip statistics clearly obeys a power law whose exponent depends on loading velocity and viscosity. We propose a simple model which explains the physical meaning of the power law exponent.

2. Experiment

2.1. Experimental apparatus

Figure 1(a) shows our experimental setup. A polymethyl methacrylate (PMMA) block (L = 30 mm (sliding direction), W = 100 mm (perpendicular to sliding direction), H = 20 mm (thickness)) with optically flat surface is connected to a load cell (force sensor) and is slid against a poly-dimethyl siloxane (PDMS) gel plate (L = 200 mm, W = 200 mm, H = 10 mm) prepared on a glass plate. The upper PMMA block and the load cell are fixed and the lower gel plate was driven at a constant velocity V, ranging from 1000 μm/s to 1 μm/s. A constant normal force F_N = 8.8 N was applied. The lateral force F acting on the block was measured by the load cell and represents the friction force. Sliding friction between the PMMA block and PDMS gel plate was not spatially uniform nor temporally steady, but proceeded by localized and sporadic interface detachment episodes of various sizes. It is the purpose of our experiments to image the spatio-temporal evolution of these detachment events which, by analogy to earthquakes, we will call also "slip events".

2.2. Sample

Two types of PDMS gels (hereafter called Gel A and Gel B) were prepared. Gel A was prepared by curing a mixture of SILPOT 184 polymer: SILPOT 184 curing agent: SE 1886 A: SE 1886 B (Toray Dow Corning, Japan) = 30 : 2 : 4 : 16 in weight fraction. For Gel B, PDMS polymer with a 5 wt% of curing agent (SILPOT 184, Toray Dow Corning, Japan) was used. After each prepolymer was stirred by an agitator, it was degassed by a vacuum pump to remove air bubbles, poured onto a flat glass plate with a mold, and cured at 120 deg for 3 hours. Rheological measurements were done using a rheometer (Anton Paar MCR301, parallel plate, d = 25 mm) for the above 2 samples. Figure 1(b) shows the results for the linear viscoelasticity at room temperature. The storage modulus (G') is almost the same for both samples ($\sim$ 0.2 MPa for all frequency ranges), while their loss modulus (G") is about one-order of magnitude different, i.e., Gel A has a less viscous character than Gel B. Though both gels are considered to include liquid components, no solvent coming out from the gel was observed for both samples during friction experiments. It suggests that the lubrication effect is negligible in our system, unlike the gel systems reported by *Baumberger et al.* [2002; 2003] (in fact, we observed the propagation of Schallamach waves [*Schallamach*, 1971] rather than self-healing slip pulses). Due to the preparation of the gels on the glass plate, strong adhesion between the gel and the bottom glass plate was maintained during experiments without any decohesion or slippage at the bottom interface.

2.3. Visualization

The spatial pattern of the slip region was observed by a simple technique shown in Figure 1(a). In this setup, since a white light is illuminated in a total internal reflection condition, slip (slightly detached) regions can be visualized as dark areas, while the stuck contact regions are bright. The images were taken by a high-vision camera (HDR-SR12, SONY, Japan) at 30 frames per second.

2.4. Determination of a slip event

In this study, we represented the size of a slip event by the force drop, which is determined by the difference between the local maxima and the first subsequent local minima in the measured friction force data (see Figure 2(b) and 3(b)). With the direct use of the raw data, however, the force drop value is largely distorted due to the existence of random experimental noise (unphysical force fluctuations). Spurious local minima due to noise can "break" up a slip event before its real end or generate false small slip events when the interface is locked and there are no slip events. In order to reduce the effects of the measurement noise on the size of slip events, we discretized the measured force data

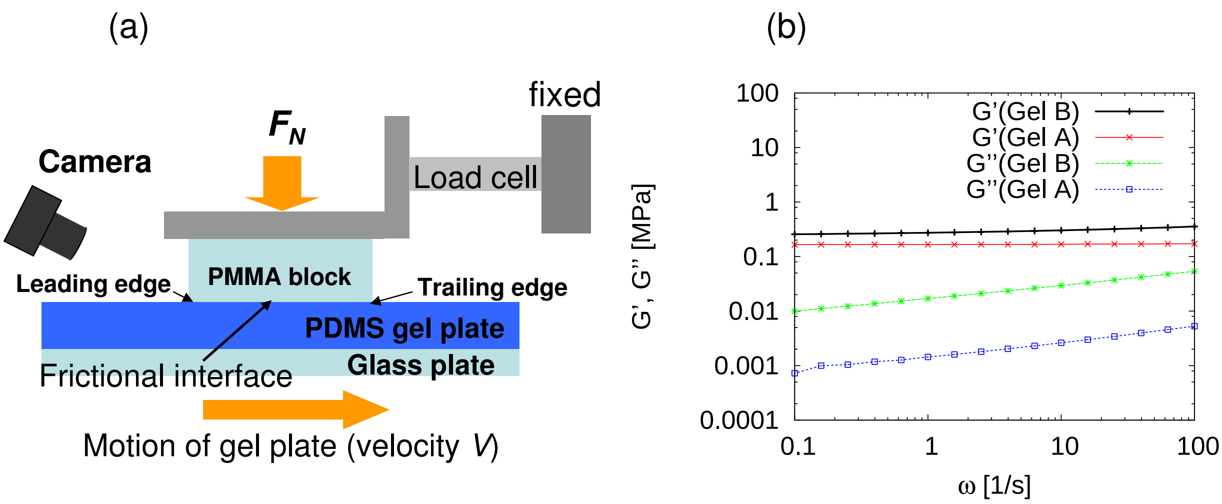

Figure 1. (a) Schematic of experimental apparatus, (b) linear viscoelasticity $G'(\omega)$ and $G"(\omega)$ at room temperature for Gel A (less viscous gel) and Gel B (more viscous gel).

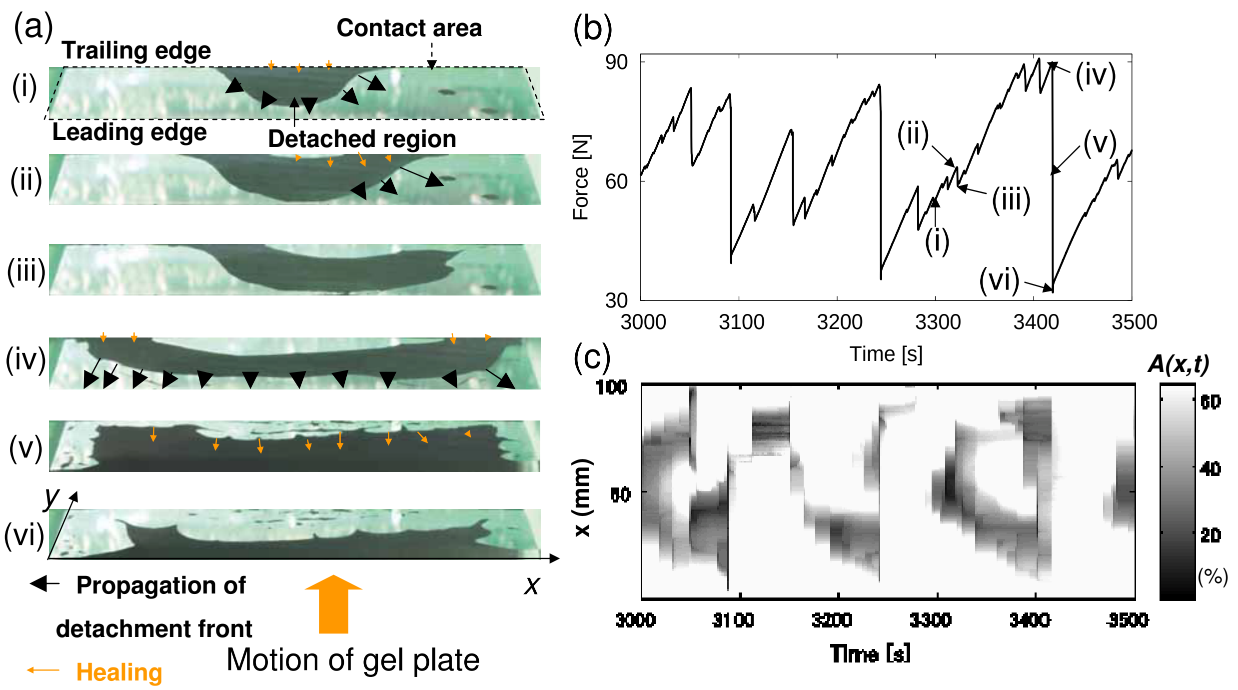

Figure 2. Slip behavior of Gel A at $V = 10$ μm/s. (a) Representative snapshots, (b) time variation of the frictional force, and (c) time variation of the average contact area $A(x,t)$ (defined in equation (1)). The numbers in (b) correspond to the images in (a).

by 0.05 N (several times larger than the noise level, see [*Yamaguchi et al.*, 2009]) by using the "round" function. We then identified all the local maxima and the local minima in the discretized force curve $F(t)$, and defined the force drop ΔF. Even after such treatment, many false events tend to be generated at small sizes. We discarded small force drop events and adopted the slip events whose force drop values are larger than 0.1 N. As a consequence, we analyzed 145, 1407, 5089, and 9178 slip events at V = 1000, 100, 10, and 1 μm/s respectively for Gel A, and 336, 1758, 8413, and 13837 events for Gel B.

3. Results and Discussion

3.1. Slip behavior

Figure 2 and 3 show representative slip events at the plate velocity $V = 10$ μm/s for the two types of gel samples, Gel A and Gel B, respectively. Each image of Figure 2(a) is a snapshot of the spatial distribution of slip for Gel A and Figure 2(b) shows the time variations of the friction force. The bright areas in Figure 2(a) correspond to the contact regions, while the dark areas are the detached regions. The gap between the two surfaces in the detached regions is roughly estimated as $\sim$ μm by the appearance of interference fringes. In Figure 2(a), a semi-circular detached region spreads with intermittent small events at the early stage ((i)-(iii)), and when the region reaches some critical size ((iv)), a large and rapid event with a sound occurs and ruptures all the remaining areas in contact. This kind of lateral propagation behavior is characteristic of our system having a 2D frictional interface. As shown in Figure 2(b), the force fluctuates during loading in the early stage ((i)-(iii)) and culminates in a large force drop during the rapid detachment event ((iv)-(vi)).

Figure 2(c) shows the time evolution of the contact area averaged over the y axis (parallel to the sliding direction),

$$A(x,t) = \frac{1}{L}\int_0^L A(x,y,t)dy, \qquad (1)$$

where L is the length of the block along the y (sliding) direction (x and y are indicated in Figure 2(a)(vi)), and $A(x,y,t)$ takes the value 100(%) if the gel is in contact with the block at (x,y) and 0 if it is detached. Thus, bright (dark) points indicate large (small) average contact areas along the y direction at a given time. Other than the spike-like patterns indicating the large and rapid propagation of detachment fronts (corresponding to large force drops in Figure 2(b)), small, intermittent and step-like events of the detached regions (corresponding to small force drops) were clearly observed prior to large slip events. These behaviors are similar to those observed for the frictional system between two PMMA blocks by *Rubinstein et al.* [2004; 2006; 2007; 2008]: the onset of large frictional motion is preceded by a discrete sequence of precursor events.

On the other hand, the slip behavior is different for the more viscous Gel B. Figure 3(a) shows the corresponding snapshots. During shearing, the detachment fronts were slowly generated at the trailing edge and propagated towards the central region (see Figure 3(a)(i) and (ii)), and were accumulated to form a large detached region shown in the pictures. Then a comparatively large event ($\Delta F \sim 15$ N) took place abruptly in the left edge of the frictional interface (see (iii)) and stopped in the middle of the contact region. At later stages, slow healing processes were observed (small arrows in (iv) and (v)). During slip events in this velocity condition, there was no sound recorded by the microphone equipped on the camera, i.e., slip events in this case are considered to be "aseismic" [*Sacks et al.*, 1978; *Rogers and*

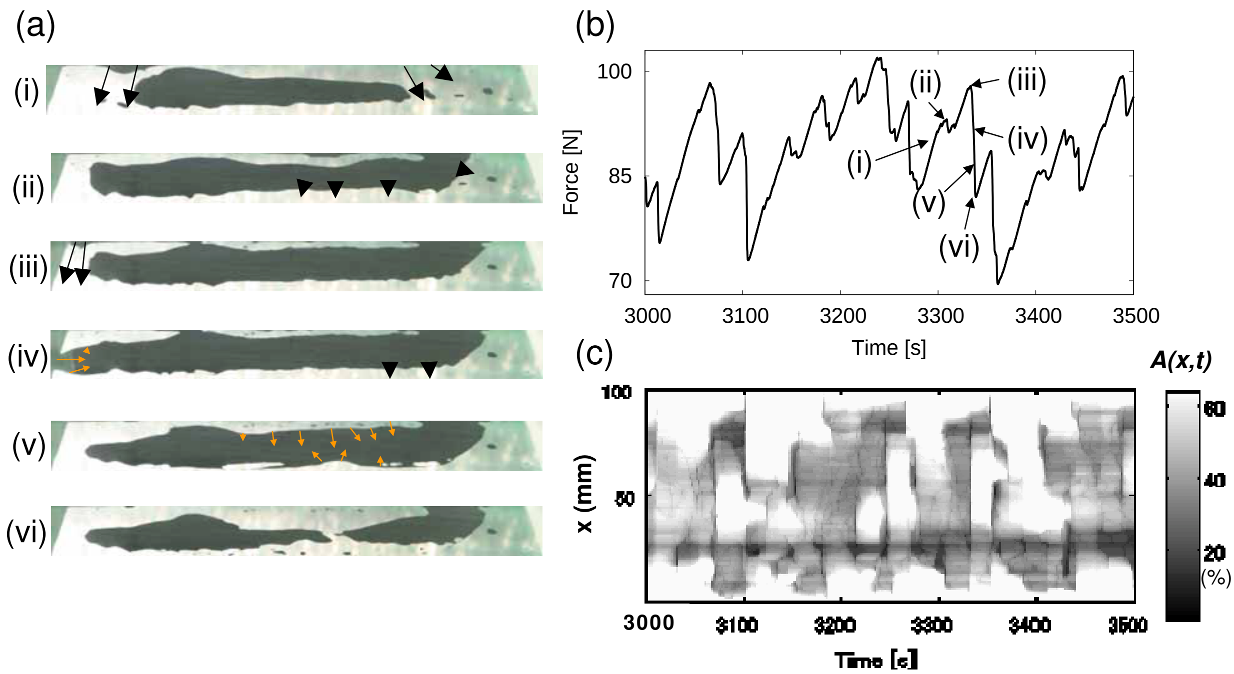

Figure 3. Slip behavior of Gel B at $V = 10$ μm/s. (a) Representative snapshots, (b) time variation of the frictional force, and (c) time variation of the average contact area $A(x, t)$ (defined in equation (1)). The numbers in (b) correspond to the images in (a).

Dragert, 2003; *Shelly et al.*, 2006; *Ide et al.*, 2007] (in order to confirm whether they are truly aseismic, it may be interesting to measure acoustic emissions). As is evident in Figure 3(b), the force fluctuations seem irregular and include frequent small slip events as well as rare large events. The statistics of the event sizes are analyzed in section 3.3.

Major differences between Gel A and Gel B appear in the spatio-temporal plots shown in Figure 2(c) and 3(c). In Gel A, a detached (dark) region nucleates and spreads in the x direction in an intermittent (step-like) manner, and abruptly disappears after a large and rapid detachment event. On the other hand, in Gel B, detached regions are always present on the interface, and successive, slow detachment motions are seen.

3.2. Statistics of force at initiation

Figure 4 shows the probability distributions of the friction force F_{ini} when a slip event is initiated. Figure 4(a) and 4(b) correspond to Gel A and B respectively, and the plate velocity V is 10 μm/s in both experiments. As shown in Figure 4(a) for Gel A, the distribution considering all slip events has a bimodal shape while the distribution considering only large events with $\Delta F > 30$ N has a single peak around 90 N. This means that, as the shear loading proceeds after a large slip event, slip becomes active at small force levels (Friction force ~ 60 N), turns less active at larger loads (~ 70 N), and finally reactivates until the next large slip event occurs (~ 90 N). At this moment, the underlying mechanisms responsible for this three-steps precursor activity are not understood and the relationship between this and the precursor behavior reported by *Rubinstein et al.* [2004; 2006; 2007; 2008] is not clear. Detailed analysis of the temporal evolution of local stress will be reported in a separate work. On the other hand, a large difference is seen in the force level statistics for Gel B as shown in Figure 4(b): unlike the bimodal distribution in Gel A, the distribution is unimodal with a peak around 90 N for all events, and a peak in the distribution for the large events appeared at a slightly larger force level than the peak position for all events.

3.3. Size distribution

In order to characterize statistics of the slip size, we plotted the cumulative distributions of the force drop ΔF for Gel A in Figure 5(a) and for Gel B in 5(b). The cumulative distribution $N(\Delta F)$ is defined by the number of events larger than ΔF divided by the total number of events we analyzed. As is seen in Figure 5, the distributions for both gels obey a power law,

$$log_{10} N(\Delta F) = -\beta log_{10} \frac{\Delta F}{\Delta F_{min}}, \quad (2)$$

where β is the exponent of the power-law distribution and $\Delta F_{min}(= 0.1$ N) is the lower cutoff of the force drop. The exponents β were determined by least squares fitting of equation (2) in the interval $\Delta F = [0.1N, 20N]$. The values were 0.10±0.01, 0.41±0.01, 0.64±0.01, and 0.74±0.01 for Gel A, and 0.099±0.001, 0.50±0.01, 0.72±0.01, and 0.92±0.02 for Gel B at $V = 1000$, 100, 10, and 1 μm/s, respectively (here we applied the single-parameter power-law fitting because it is rather simple but roughly captures the physics, i.e., the relative frequency of large events and the resulting average force drop value are characterized by β, as discussed later). The results indicate that the exponent β is dependent not only on the plate velocity, but also on the viscosity of the gel. These variations in the exponent are reminiscent of the elastic parameter α in the OFC model [*Christensen and Olami*, 1992; *Olami et al.*, 1992], and their physical meaning will be discussed in section 3.5.

Here it is important to note two points. First, small precursor events prior to large catastrophic events (seen in Figure 2(a)) constitute the power-law statistics [*Carlson*, 1989; *Stirling*, 1996] for Gel A (see Figure 5(a)). Second, as shown

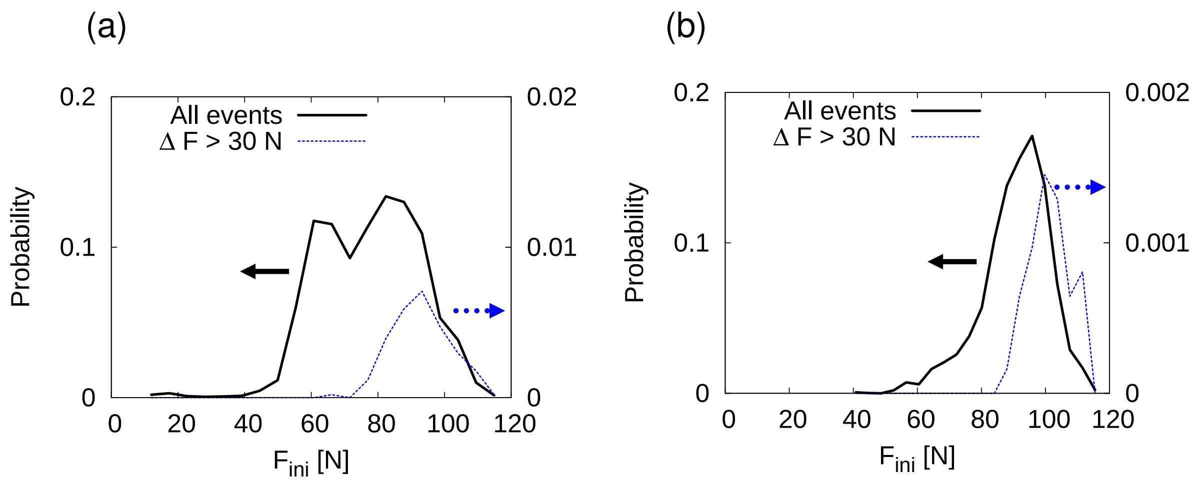

Figure 4. Probability distributions of the friction force at event initiation at $V = 10$ μm/s for Gel A (a) and Gel B (b). Solid line denotes the distribution for all slip events (left axis) and dotted line for large events ($\Delta F > 30$ N, right axis). For each plot, 20 bins are used.

in Figure 5(b), the size distributions for Gel B at small plate velocities "bend" at an intermediate force drop ($\Delta F \sim 5$N) and the number of the large events looks smaller than those expected from the (single exponent) power-law distribution. This might be a consequence of the suppression of the dynamic frictional weakening [*Ben-Zion et al.*, 2003; *Dahmen et al.*, 2011] due to viscoelastic dissipation.

Finally, let us discuss the relationship between the b value and the exponent β. Since the force drop is approximately proportional to the earthquake seismic moment M_0 for our "thin" gels:

$$\Delta F \approx \frac{\mu D A}{H} \propto \mu D A = M_0 \tag{3}$$

where μ, D, H, and A being the modulus, the slip, the thickness of the gel, and the rupture area respectively, the following relation holds:

$$\begin{aligned} log_{10}N(\Delta F) &= a - bM = a - \frac{2b}{3}(log_{10}M_0 - 9.1) \\ &= a' - \beta log_{10}\Delta F, \end{aligned} \tag{4}$$

where a and a' are the normalization constants. From equation (4), we have $\beta = 2b/3$. For example, $b = 1$ corresponds to $\beta = 2/3 \approx 0.67$.

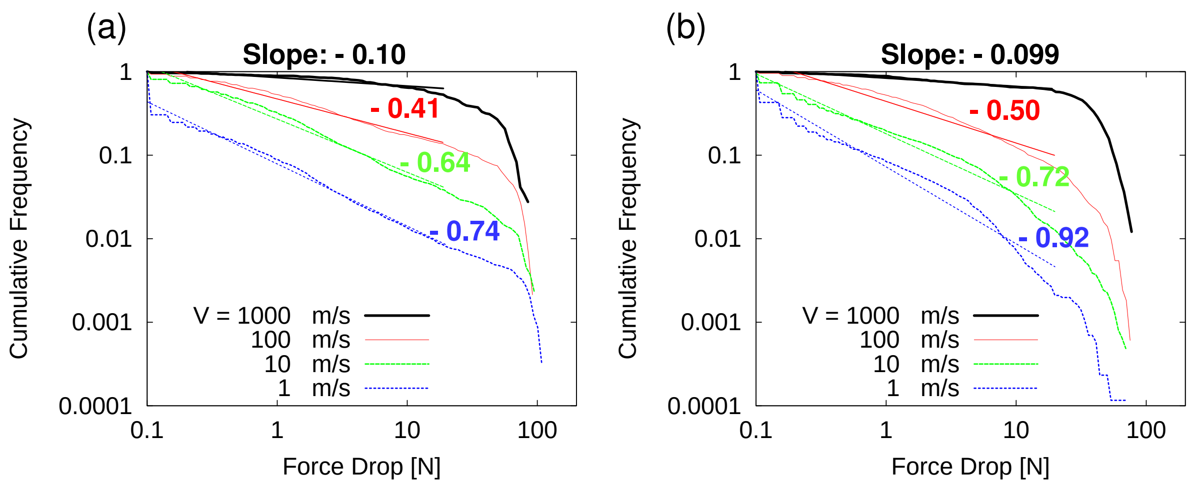

Figure 5. (a) Cumulative frequency plots of the force drop for (a) Gel A and (b) Gel B at 4 different plate velocities. Each frequency is normalized by the total number of events. For each plot, 100 bins are used and a power-law fitting curve is also drawn.

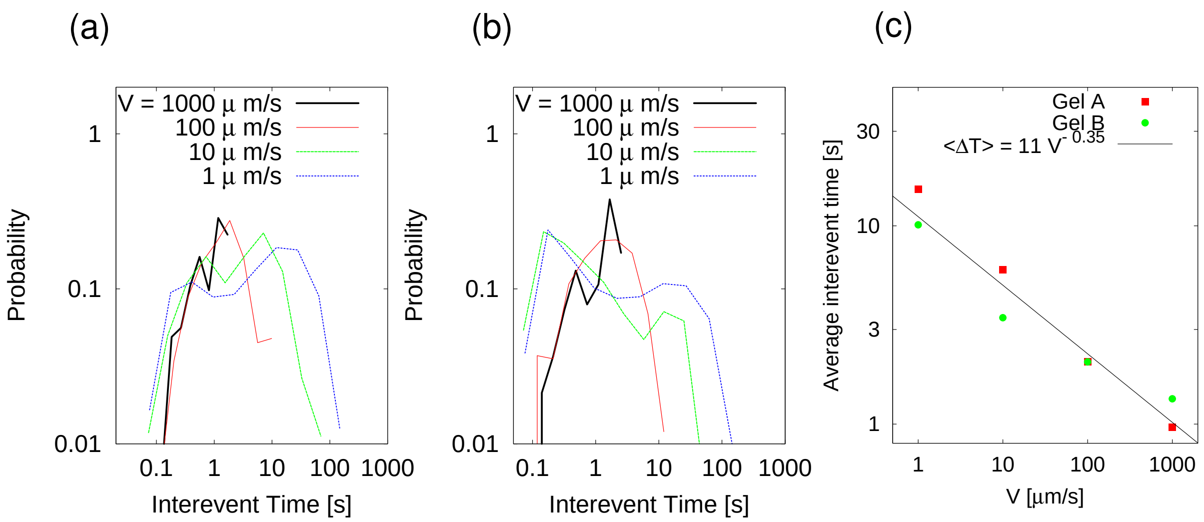

Figure 6. Interevent time distributions for Gel A (a) and Gel B (b) at four different plate velocities. 10 bins are used for each plot. (c) Plate velocity dependence on the average interevent time $< \Delta T >$. The fitting curve (equation (5)) is also drawn in the figure.

3.4. Interevent time distribution

Figure 6(a) and 6(b) show the distributions of interevent times (the time intervals between successive slip events) in Gel A and Gel B, respectively. In both gels, the distributions extend towards longer interevent times at smaller plate velocities. In order to characterize their behavior, the average interevent time is plotted against the plate velocity V in Figure 6(c). The least squares fitting by a power law

$$< \Delta T > = < \Delta T >_0 (\frac{V}{V_0})^{-\alpha} \quad (5)$$

with reference speed $V_0 = 1$ μm/s results in $\alpha = 0.35$ and $< \Delta T >_0) = 11$ s. The effect of the viscosity of the gels is mild. The result is in contrast with shear experiments of granular matter [*Nasuno et al.*, 1998], in which the average interevent time is inversely proportional to the driving velocity ($\alpha = 1$, i.e., the events are determined by displacements of the plate, not by time). The reason for the weak dependence of the average interevent time on the plate velocity and on the type of gel is not clearly understood but might be explained by the effect of viscoelastic relaxation.

3.5. Simple model

In order to describe the dependence of the exponent β on plate velocity V, we consider a simple model. We first assume a steady-state condition, where the force increase due to shear deformation of the contact (stuck) region is compensated by slip events. This assumption is expressed by

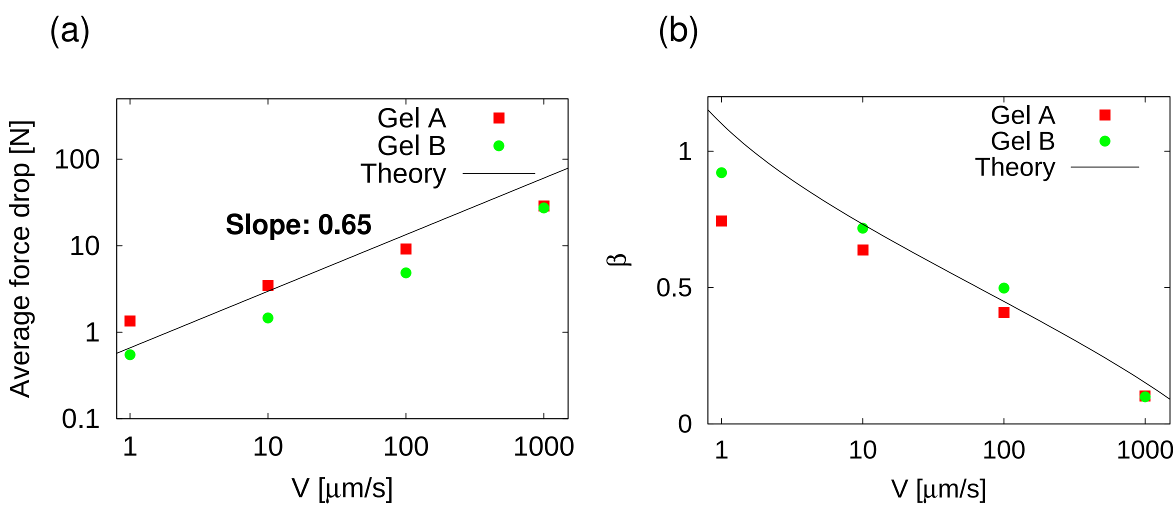

Figure 7. Plate velocity dependence on (a) average force drop $< \Delta F >$ and (b) power-law exponent β. Theoretical curves (equation (7) and (10)) are also drawn in the figures. Note that the error bars in β were smaller than the size of the points (~ 0.05).

the following equation.

$$< \Delta F >= \frac{\mu V < \Delta T > S}{H}, \quad (6)$$

where $< \Delta F >$ is the average value of the force drop, μ (= 0.2 MPa) is the shear modulus of the gel, $< \Delta T >$ is the average interevent time (equation (5)), $H(= 1 \times 10^{-2}$ m) is the thickness of the gel, and $S(= 3 \times 10^{-3} m^2)$ is the nominal contact area of the block. Substituting equation (5) into (6),

$$< \Delta F >= \frac{\mu V_0 < \Delta T >_0 S}{H} (\frac{V}{V_0})^{1-\alpha}. \quad (7)$$

Figure 7(a) shows our results for the dependence of the average force drop on plate velocity and the theoretical curve $< \Delta F >= 0.66(V/V_0)^{0.65}$ calculated from equation (7). Though our simple theory overestimates the average force drop at large plate velocities, it qualitatively explains the observed behavior.

Next, we introduce a power law distribution for the probability density function $P(\Delta F)$.

$$\begin{aligned} P(\Delta F) d(log_{10} \Delta F) &= \frac{dN(\Delta F)}{d(log_{10} \Delta F)} d(log_{10} \Delta F) \\ &= C \Delta F^{-\beta} d(log_{10} \Delta F), \quad (8) \end{aligned}$$

where $C = (\beta ln 10)/(\Delta F_{min}^{-\beta} - \Delta F_{max}^{-\beta})$ is the normalization constant and ΔF_{max} is the upper cutoff of the force drop. The expected value of the force drop can be calculated with this probability density function,

$$< \Delta F >= \Delta F_{min} \frac{\beta}{1-\beta} \frac{R^{1-\beta} - 1}{1 - R^{-\beta}}, \quad (9)$$

where $R = \Delta F_{max}/\Delta F_{min}$ is the ratio between the upper and the lower cutoff of the force drop. Assuming ΔF_{max} and ΔF_{min} are constant, equation (9) is a monotonously decreasing function for β [*Ramos*, 2011].

By equating the right hand sides of equation (7) and (9), we obtain the following relation,

$$V = V_0 \{ \frac{H \Delta F_{min}}{\mu V_0 < \Delta T >_0 S} (\frac{\beta}{1-\beta}) \frac{R^{1-\beta} - 1}{1 - R^{-\beta}} \}^{1/(1-\alpha)}. \quad (10)$$

Figure 7(b) shows the dependence of β on plate velocity and the theoretical curve (equation (10)) with an adjustable parameter $R = 10^4$ to obtain a best fit. The theoretical curve is in good agreement with experimental observations though there are some deviations at small plate velocities. This result suggests that the power-law exponent β is simply related to the average size of the event through equation (9): i.e., larger events tend to occur more often at large plate velocities than at small plate velocities.

In the above discussions, we considered a simple model to explain dependence of the β value on the plate velocity. However, the mechanisms responsible for the plate velocity dependence may be understood in an intuitive manner: since our gel materials are viscoelastic and far from the glassy state, as shown in Figure 1(b), the propagation of detachment fronts is characterized by rate-dependent, velocity-strengthening fracture energy [*Gent*, 1996; *de Gennes*, 1996; *Persson et al.*, 2005; *Yamaguchi et al.*, 2009]. In the previous studies by the authors [*Yamaguchi et al.*, 2009], the maximum strain stored inside the gel increases with increasing plate velocity, and larger stress drop during detachment is obtained. As a result, the average force drop, which is given by the stress drop times rupture area becomes larger and the β value becomes smaller with increasing plate velocity.

On the other hand, explanations for the difference in the exponent β between the gels need some discussion. One explanation is that, since the work done by shearing is more strongly dissipated inside Gel B than inside Gel A, larger part of the stored elastic energy to drive rupture is lost and thus smaller slip events are generated for Gel B than for Gel A. Another explanation is that, dynamic weakening of the frictional strength is more strongly suppressed due to the damping of emitted elastic waves for the more viscous Gel B than for the less viscous Gel A. Both explain larger exponents for Gel B than for Gel A.

4. Conclusion

We studied spatio-temporally heterogeneous stick-slip motions in the sliding friction between a hard PMMA block and soft PDMS gels with two different viscoelastic properties. We observed different slip behaviors: for the less viscous gel, larger and more rapid events occurred and a bimodal distribution of the force at initiation of a slip event was observed, while for the more viscous gel, slower and smaller slip events took place. The probability distributions of the force drop obey a power law for both gels and the exponent depends on the plate velocity and on the viscosity. We proposed a simple model to explain these dependencies and found a good agreement with experimental results.

Though this experiment suggests a potential possibility for an analogue model of an earthquake system, many studies remain to be done. For example, the elementary process or constitutive law for the rupture process in gels are still unexplored and further investigations measuring local stress or displacement fields are needed. More detailed analysis on fast rupture processes with high speed cameras are also needed. Furthermore, the mechanisms responsible for the power law behavior is not well understood. These are research topics for future study.

Acknowledgments. We thank T. Hatano, S. Ide, H. Kitahata and Y. Sumino for valuable comments.

References

Bak, P., C. Tang, and K. Wiesenfeld, Self-organized criticality: An explanation of the 1/f noise, *Phys. Rev. Lett., 59*, 381–384, 1987.

Baumberger, T., C. Caroli, and O. Ronsin, Self-healing slip pulses along a gel/glass interface, *Phys. Rev. Lett., 88*, 075509-1–4, 2002.

Baumberger, T., C. Caroli, and O. Ronsin, Self-healing slip pulses and the friction of gelatin gels, *Eur. Phys. J. E, 11*, 85–93, 2003.

Ben-Zion, Y., M. Eneva, and Y. Liu, Large earthquake cycles and intermittent criticality on heterogeneous faults due to evolving stress and seismicity, *J. Geophys. Res., 108*, 2307, 2003.

Bretz, M., R. Zaretzki, S. B. Field, N. Mitarai, and F. Nori, Broad distribution of stick-slip events in slowly sheared granular media: Table-top production of a Gutenberg-Richter-like distribution, *Europhys. Lett., 74*, 1116–1122, 2006.

Burridge, R., and L. Knopoff, Model and theoretical seismicity, *Bull. Seism. Soc. Am., 57*, 341, 1967.

Carlson, J. M., and J. S. Langer, Properties of earthquakes generated by fault dynamics, *Phys. Rev. Lett., 62*, 2632–2635, 1989.

Christensen, K., and Z. Olami, Scaling, phase transitions, and nonuniversality in a self-organized critical cellular-automaton model, *Phys. Rev. A, 46*, 1829–1838, 1992.

Ciliberto, S., and C. Laroche, Experimental evidence of self organized criticality in the stick-slip dynamics of two rough elastic surfaces, *J. Phys. I France, 4*, 223–235, 1994.

Dahmen, K. A., Y. Ben-Zion and J. T. Uhl, A simple analytic theory for the statistics of avalanches in sheared granular materials *Nature Phys., 7*, 554–557, 2011.

Dalton, F., and D. Corcoran, Self-organized criticality in a sheared granular stick-slip system, *Rhys. Rev. E, 63*, 061312-1–4, 2001.

de Gennes, P. G., Soft adhesives, *Langmuir, 12*, 4497–4500, 1996.

Dieterich, J. H., Time-dependent friction and the mechanics of stick-slip, *Pure Appl. Geophys., 116*, 790–806, 1978.

Dieterich, J. H., Modeling of rock friction 1. experimental results and constitutive equations, *J. Geophys. Res., 84*, 2161–2168, 1979.

Gent, A. N., Adhesion and strength of viscoelastic solids. Is there a relationship between adhesion and bulk properties ?, *Langmuir, 12*, 4492–4496, 1996.

Gutenberg, B., and C. F. Richter, *Seismicity of the earth and associated phenomena*, Hafner Publishing Company, New York and London, 1965.

Ide, S., G. C. Beroza, D. R. Shelly, and T. Uchide, A scaling law for slow earthquakes, *Nature, 447*, 76–79, 2007.

Marone, C., The effect of loading rate on static friction and the rate of fault healing during the earthquake cycle, *Nature 391*, 69–72, 1998.

Mogi, K., Regional variations in magnitude-frequency relation of earthquakes, *Bull. Earthq. Res. Inst., 45*, 313–325, 1967.

Mori, J., and R. E. Abercrombie, Depth dependence of earthquake frequency-magnitude distributions in California: Implications for rupture initiation, *J. Geophys. Res., 102*, 15081–15090, 1997.

Morishita, M., M. Kobayashi, T. Yamaguchi, and M. Doi, Observation of spatio-temporal structure in stick-slip motion of an adhesive gel sheet, *Journal of Physics: Condensed Matter, 22*, 365104-1–6, 2010.

Nasuno, S., A. Kudrolli, A. Bak, and J. P. Gollub, Time-resolved studies of stick-slip friction in sheared granular layers, *Phys. Rev. E, 58*, 2161–2171, 1998.

Olami, Z., H. J. S. Feder, and K. Christensen, Self-organized criticality in a continuous, nonconservative cellular automaton modeling earthquakes, *Phys. Rev. Lett., 68*, 1244–1247, 1992.

Persson, B. N. J., *Sliding Friction: Physical Principles and Applications*, Springer, New York, 2000.

Persson, B. N. J., O. Albohr, G. Heinrich, and H. Ueba, Crack propagation in rubber-like materials, *J. Phys.: Condens. Matter, 17*, R1071–1142, 2005.

Ramos, O., Scale invariant avalanches: a critical confusion, *Horizons in Earth Science Research, vol.3,*, B. Veress and J. Szigethy (eds.), Nova Science Publishers, Inc., 157–188, 2011.

Rogers, G., and H. Dragert, Episodic tremor and slip on the Cascadia subduction zone: the chatter of silent slip, *Science, 300*, 1942–1943, 2003.

Rubinstein, S. M., G. Cohen, and J. Fineberg, Detachment fronts and the onset of dynamic friction, *Nature, 430* 1005–1009, 2004.

Rubinstein, S. M., M. Shay, G. Cohen, and J. Fineberg, Crack-like processes governing the onset of frictional slip, *Int. J. of Fracture, 140*, 201–212, 2006.

Rubinstein, S. M., G. Cohen, and J. Fineberg, Dynamics of Precursors to Frictional Sliding, *Phys. Lett. Rev. 98*, 226103-1–4, 2007.

Rubinstein, S. M., G. Cohen, and J. Fineberg, Cracklike processes within frictional motion: Is slow frictional sliding really a slow process ?, *MRS Bulletin 33*, 1181–1189, 2008.

Ruina, A. L., Slip instability and state variable friction laws, *J. Geophys. Res., 88*, 10359–10370, 1983.

Sacks, I. S., S. Suyehiro, A. T. Linde, and J. A. Snoke, Slow earthquakes and stress redistribution, *Nature, 275*, 599–602, 1978.

Schallamach, A., How does rubber slide ?, *Wear, 17*, 301–312, 1971.

Scholz, C. H., Earthquakes and friction laws, *Nature, 391*, 37–42, 1998.

Scholz, C. H., *The Mechanics of Earthquakes and Faulting, 2nd ed.*, Cambridge University Press, Cambridge, 2002.

Schorlemmer, D., S. Wiemer, and M. Wyss, Variations in earthquake-size distribution across different stress regimes, *Nature, 437*, 539–542, 2005.

Shelly, D. R., G. C. Beroza, S. Ide and S. Nakamula, Low-frequency earthquakes in Shikoku, Japan, and their relationship to episodic tremor and slip, *Nature, 442*, 188–191, 2006.

Stirling, M. W., S. G. Wesnousky, K. Shimazaki, Fault trace complexity, cumulative slip, and the shape of the magnitude-frequency distribution for strike-slip faults: a global survey, *Geophys. J. Int., 124*, 833–868, 1996.

Strogatz, S. H., *Nonlinear Dynamics and Chaos,* Westview, 1994.

Utsu, T., Space-time pattern of large earthquakes occurring off the Pacific coast of the Japanese islands, *J. Phys. Earth, 22*, 325–342, 1974.

Vallette, D. P., and J. P. Gollub, Spatiotemporal dynamics due to stick-slip friction in an elastic-membrane system, *Phys. Rev. E, 47*, 820–827, 1993.

Yamaguchi, T., S. Ohmata, and M. Doi, Regular to chaotic transition of stick-slip motion in sliding friction of an adhesive gel-sheet, *Journal of Physics: Condensed Matter, 21*, 205105-1–7, 2009.